

This file has been cleaned of potential threats.

If you confirm that the file is coming from a trusted source, you can send the following SHA-256 hash value to your admin for the original file.

df147fec23cdb25fcc21682060181d358f5d470d256f6c228bfc66b31be77ed9

To view the reconstructed contents, please SCROLL DOWN to next page.

Opto-electrical properties of amorphous carbon thin film deposited from natural precursor camphor

Debabrata Pradhan^{*}, Maheshwar Sharon

Department of Chemistry, Indian Institute of Technology Bombay, Mumbai 400 076, India

Received 27 November 2006; received in revised form 3 February 2007; accepted 6 February 2007

Available online 15 February 2007

Abstract

A simple thermal chemical vapor deposition technique is employed for the pyrolysis of a natural precursor “camphor” and deposition of carbon films on alumina substrate at higher temperatures (600–900 °C). X-ray diffraction measurement reveals the amorphous structure of these films. The carbon films properties are found to significantly vary with the deposition temperatures. At higher deposition temperature, films have shown predominately sp^2 -bonded carbon and therefore, higher conductivity and lower optical band gap (Tauc gap). These amorphous carbon (a-C) films are also characterized with Raman and X-ray photoelectron spectroscopy. In addition, electrical and optical properties are measured. The thermoelectric measurement shows these as-grown a-C films are p-type in nature.

© 2007 Elsevier B.V. All rights reserved.

PACS : 81.05.Gc; 73.61.Jc; 78.30.-j; 73.50.Lw; 78.20.-e

Keywords: Camphor; a-C films; Raman spectroscopy

1. Introduction

Although synthesizing artificial diamond is a technological challenge, the so obtained material is not much cheaper than the natural one. Therefore, it is quite understandable why there was euphoria among scientific community on the first discovery of diamond like carbon (DLC) [1]. Aisenberg and Chabot had coined this particular metastable form of carbon as diamond like carbon (DLC) due to its properties similar to diamond [1]. Thereafter, different names have been used for similar films of DLC while the same name has been used to describe entirely different films, e.g. i-C (ion assisted carbon films), H-carbon (hydrogenated carbon films) [2], a-C (amorphous carbon) [3,4], a-C:H (hydrogenated amorphous carbon in both hard and soft form) [5], ta-C (tetrahedral amorphous carbon), ta-C:H (tetrahedral hydrogenated amorphous carbon) films [6], etc. This inconsistent nomenclature is primarily due to the broad

spectrum of properties and variety of methods used for preparing the carbon films [7]. Diamond and graphite have completely 100% sp^3 and sp^2 network in their lattice, respectively. Inter-mediating percentage of sp^3 and sp^2 has been found in the examples given above. The important properties of any such carbon films are mapped by the methods used for deposition, sp^3/sp^2 ratio, % of hydrogen, disorderliness in the films, etc. With the superior properties of carbon films (having high sp^3 percentage) such as micro-hardness like sapphire, low frictional coefficient, inertness to any aggressive chemical and also ability to coat geometrically complex bodies; these carbon films can be used in the applications like antisticking overcoats for computer disks [8], anticorrosive coating for surgical instruments [9], solar cells [10,11], electron field emission [12,13] and electrodes in electrochemical reactions [14], etc. It is worthwhile to mention that the nature and properties of carbon films play an important role in various applications.

In the present study, a simple thermal chemical vapor deposition (CVD) technique is adopted for the preparation of carbon films from a natural precursor “camphor ($C_{10}H_{16}O$)” unlike plasma CVD (PECVD, MPCVD, PLD, etc.) that are commonly used for the deposition of various types of carbon

^{*} Corresponding author. Present address: Department of Chemistry, University of Waterloo, 200 Univ. Avenue West, Waterloo, Ontario N2L 3G1, Canada. Tel.: +1 519 888 4567x37763; fax: +1 519 746 0435.

E-mail address: dpradhan@sciborg.uwaterloo.ca (D. Pradhan).

films [7]. It is worth noting that for deposition on complex geometrical structures and large sized substrate, thermal CVD is an ideal choice. In the preparation of carbon films, a high percentage of sp^3 bonded carbon atoms is preferred in crystal lattice. Use of camphor as a precursor for depositing carbon film could be more favorable than any other precursors because a single camphor molecule contains nine sp^3 -bonded carbon. At the same time, one oxygen atom inside the camphor molecule could help in oxidizing some non-diamond like carbons during deposition. This is a novel precursor that we have used to deposit amorphous carbon (a-C) films in the present study unlike methane or acetylene or graphite target normally used for same [15]. Additionally, lower H/C ratio in case of camphoric gas has another advantage in producing lower hydrogen contents in the film compared to methane gas. We have previously synthesized various carbonaceous materials, e.g. fullerene [16], spongy carbon beads [17], carbon nanotube [18], carbon nanofibers [19,20] using camphor as precursor. Besides precursor there are many other deposition parameters that decide sp^3/sp^2 carbon ratio in the carbon films. As the correct terminology used to designate the different types of carbon films of different sp^3/sp^2 ratio is still being ambiguous, we designate “amorphous carbon (a-C)” to the films obtained by pyrolysis of camphor as these films are found to be amorphous structure by X-ray diffraction study.

2. Experimental

2.1. Films deposition

The deposition unit consisted of a quartz tube (1.5 m long and 0.025 m in diameter), an electric furnace and an argon gas cylinder. The quartz tube was kept inside a horizontal tubular furnace. In the center of quartz tube, an alumina substrate (over which camphor is to be pyrolysed and deposited) was placed. Prior to deposition of carbon films on alumina substrate, the whole deposition chamber was purged with argon for at least 15 min. Then the temperature of electric furnace was elevated from room temperature to desired deposition temperature under argon atmosphere. Once the substrate reached the desired temperature, camphor (2 g) was vaporized at $\sim 300^\circ\text{C}$ and the vaporized gas was allowed to pass inside the quartz tube having a set temperature of 650, 700, 750 and 900°C . The evaporation of 2 g of camphor and deposition normally take around 6–12 min. However, the substrate was kept at that high temperature for 1 h and then furnace was cooled down to room temperature in same argon medium.

2.2. Characterization

Raman spectra of deposited carbon films were taken using an Ar-laser of wavelength 514.5 nm at 20 mW power. A $100\times$ objective lens was used to observe micro-Raman spectra with an illumination spot size of $1\ \mu\text{m}$ and acquisition time of 90 s in a Ramanor T64000 (Jobin Yvon) instrument. X-ray photoelectron spectroscopic (XPS) study was done with a VAMAS Surface Chemical Analysis, VG Scientific, EscaLab 220-IXL

apparatus using an aluminum K-alpha source at 1486.6 eV. The high-resolution spectra of carbon (C 1s peak), was recorded in the fixed analyzer transmission (FAT) mode. The experimental data were then fitted to peak fitting program (CASA-XPS) for distinguishing different carbon peaks. X-ray diffraction (XRD) was carried out with Philips PW1729 X-ray generator using $\text{Cu K}\alpha$ ($\lambda = 1.54\ \text{\AA}$). The optical gap was measured by home fabricated spectrophotometer in the range of 400–1200 nm using a tungsten–halogen lamp. The absorbance spectrum was collected using a germanium detector. To measure the electrical resistance, two platinum wires were bound to both ends (kept 1 cm apart) of the alumina plate on which carbon film deposited. Resistance of a-C films versus temperature was measured in argon atmosphere.

3. Results and discussion

3.1. Raman spectroscopic studies

Raman spectroscopy is a prime technique for the analysis of bonding types, domain size, internal stress, etc. in carbon film [21]. The Raman peak shapes, positions, shifts, half-width and intensity give all the detailed information about the chemistry and structure of carbon films. Inelastic, incoherent Stokes Raman scattering of light from the lattice of diamond was first observed by Ramaswamy [22] and investigated in detail by Solin and Ramdas [23]. The 1st order zone center sharp Raman peak of diamond and graphite lies at 1332.5 ± 0.5 and $1580 \pm 0.5\ \text{cm}^{-1}$, respectively. All other types of carbon show broad peaks between 1100 and $1600\ \text{cm}^{-1}$ [24,25]. Fig. 1 shows the Raman spectra of a-C films obtained at different deposition temperatures. The amorphous nature of as-grown carbon films was confirmed from the X-ray diffraction (XRD) study. The Raman spectra are deconvoluted by the Gaussian peak-fitting method. Two broad bands observed at ~ 1340 and $1580\ \text{cm}^{-1}$ were named D-band (disorder/defect band) and G-band (graphitic band or E_{2g2} mode), respectively. These two bands are commonly observed in a-C films [3,26]. These bands are also observed in glassy carbon. Interestingly, in most cases the intensity of the D-band is higher than the G-band in glassy carbon [24,25,27]. Raman spectra of camphor pyrolysed films are found very similar to a-C films containing 60% sp^2 -bonded carbon [3,28]. Another prominent broad peak that observed in the range of 1540 – $1560\ \text{cm}^{-1}$ can be attributed to sp^2 -bonded carbon normally observed in the grain boundaries of diamond films at $1520\ \text{cm}^{-1}$ [29]. The D-band intensity is found to increase markedly with the deposition temperature indicating increase of disorderliness in the film. The disorderliness in the a-C films originated from micro-crystalline disordered graphite due to intermingling of σ -(sp^3 -like) domains in the clusters of π -(sp^2 -like) graphite. Tuinstra and Koenig had explained it to be due to decrease in the size of microcrystalline graphitic domains and based on X-ray analysis proposed for graphite [30]. However, Tarmor et al. ruled out this fact for a-C from optical measurements [31]. Another explanation could be a transformation of a-C types of films to nano-crystalline glassy carbon [32]. In the present study, we observed increase in the

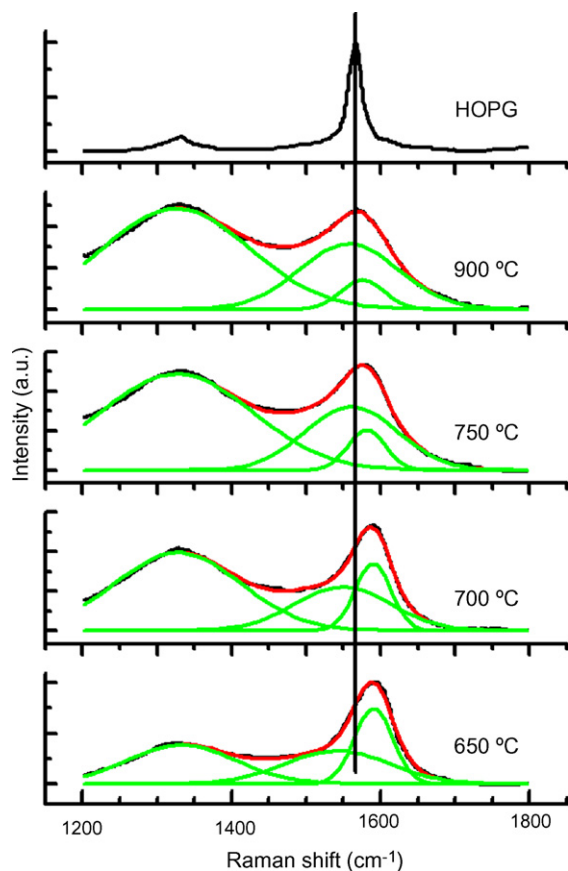


Fig. 1. Raman spectra of as grown a-C films deposited at various temperatures (HOPG: highly oriented pyrolytic graphite).

sp^2 -bonded carbons from X-ray photoelectron spectroscopic studies and lowering in band gap with increase in the deposition temperature. This clearly suggests the increase in graphitic contents along with disorderliness in the films prepared at higher deposition temperature. In the Raman spectra, it is also interesting to observe significant G-band shift with deposition temperature which is related to the stress in the film [29,33,34]. The shift of G-peak to higher wave number under applied stress obeys following equation [29].

$$\Delta(\text{G-peak position shift}) = 5 [\text{cm}^{-1}/\text{GPa}] \times [\text{GPa}] \quad (1)$$

Table 1 summarizes the ratio of D- peak to G-peak, peak position and the stress in the film calculated from Eq. (1). The decrease of stress in the film prepared at higher deposition temperature can be either due to clustering sp^2 components in

the film or by sp^3 to sp^2 transformation and followed by clustering [35].

3.2. X-ray photoelectron spectroscopic (XPS) studies

Two sets of X-ray photoabsorption studies were done with the samples deposited at various temperatures. In the first set, spectra were collected without etching top surface layers. In the second set, 10 nm of the film surface was etched-out by Ar^+ beam and then spectra were taken. As the binding energy value for both sp^3 and sp^2 carbon (C 1s) are very close, it is difficult to measure the accurate percentage of sp^3 and sp^2 by XPS. However, broad peak observed in the range of 282–290 eV were de-convoluted and fitted to original spectrum and percentage of sp^2 , sp^3 and other species were calculated from the de-convoluted peaks. Fig. 2 shows the de-convoluted X-ray photo-absorption peak of etched carbon film deposited at different temperatures. The peak at around 284.6 and ~ 285.0 eV was considered for sp^2 and sp^3 bonded carbon, respectively [36,37]. Atomic percentage of sp^3 , sp^2 and C–O bonding obtained from the XPS graphs is shown in Table 2. As expected, there was an overall increase of sp^2 -bonded carbon with deposition temperature. Low atomic percentage of sp^3 bonded carbon at high temperature deposition could be due to fragmentation of camphor molecules and rearrangement of those as sp^2 -bonded carbon structure because sp^2 -bonded carbon are thermodynamically more stable to sp^3 . However, at lower deposition temperature (650 °C), complete fragmentations and rearrangement of carbon does not occur and thereby, many sp^3 bonded carbon remains which leads to higher sp^3 atomic percentage. However, sp^2 percentage was found to be higher in all as-grown carbon films compared to etched films (etching was done inside XPS chamber). This suggests that as-grown a-C films are mostly terminated by sp^2 -bonded carbon. Percentage of sp^3 bonded carbon atom in camphor pyrolysed films are close to the value reported by Kulik et al. [28]. They measured sp^3 percentage by near K-edge EELS. Raman spectra of their films were comparable to Raman spectra of camphor pyrolysed films as well. Secondly, the C=O, C–O bonded carbon was high at lower deposition temperature which supports the partial fragmentation of camphor molecules. The carbon–oxygen percentage reduces linearly with increase in deposition temperature.

3.3. Optical properties

Optical properties of as-grown carbon films were studied in the range of 400–1200 nm. From the diffuse reflectance spectroscopy, absorbance of the deposited carbon films in the

Table 1

Position of the G-peak of the carbon films deposited by thermal CVD, the shift of the peak from the value measured in HOPG, the ratio of D- to G-peak, and stress in the films calculated according to Eq. (1)

Sample	Position of G-peak (cm^{-1})	Shift of G-peak from HOPG	I_D/I_G	Calculated stress (GPa)
650 °C	1590.3	23.8	0.51	4.7
700 °C	1589.7	23.2	1.15	4.64
750 °C	1581.0	14.5	2.37	2.9
900 °C	1575.6	9.1	3.39	1.82
HOPG	1566.5			

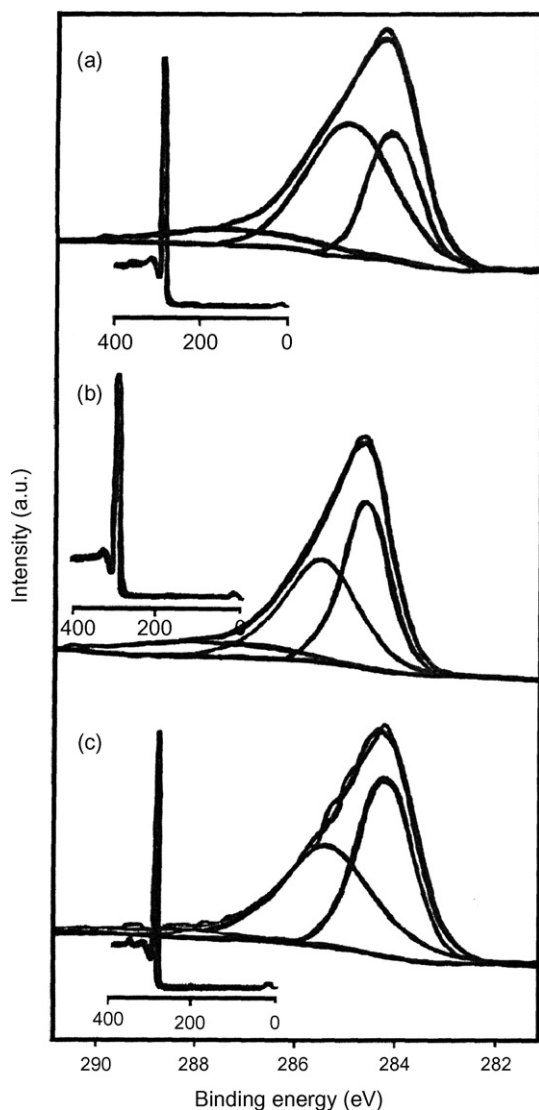


Fig. 2. XPS spectra from surface etched carbon films deposited at (a) 650 °C, (b) 750 °C and (c) 900 °C.

wavelength region of 400–1200 nm was measured. From the absorption data, the Tauc band gap of the films was estimated using the formula [6,38]:

$$\alpha h\nu = A(h\nu - E_g)^{n/2} \quad (2)$$

where $n = 1$ for a direct and $n = 4$ for an indirect band gap.

Fig. 3a and b shows the direct and indirect band gap spectra of a-C films deposited at different pyrolysis temperatures, respectively. The steep region of each spectrum is extended and the point where straight line meets the energy axis is taken as optical Tauc gap and is displayed in Table 3. It is observed that energy gap decreases with increase in the deposition temperature. Since the band gap is determined by the π -states of the sp^2 sites as these states lie closest to the Fermi level (E_f), dependence of the optical gap on the sp^2 fraction may be known from the electronic structure of a-C [39]. The fraction and arrangement of the sp^2 sites are important in influencing the optical and electronic properties of solids. It has been proposed that the sp^2 sites pair up to form π -bonds and segregate into clusters within the sp^3 matrix [39]. The formation of the clusters is opposed by disorder in the film [40]. If the disorder is low, the width of the π -bond depends on the cluster size such that the optical gap varies inversely to the cluster size. Which indicates the band gap depends on the cluster size and local distortions of the π -bonding [6,41]. However, it is now believed that any sp^2 clusters are relatively small [40]. Moreover, in this case, carbon films deposited at lower pyrolysis temperature (650 °C) have less disorderliness (see I_D/I_G ratio in Fig. 1) and have higher sp^3 bonded carbon compared to carbon films deposited at higher temperature (as measured by XPS). With increase in deposition temperature, not only disorderliness but also sp^2 percentage increases that lead to the narrow band gap. It is well known that, HOPG (highly oriented pyrolytic graphite) pyrolysed at very high temperature have zero gap and no disorderliness inside it. This suggests that percentage of sp^2 plays significant role in reducing band gap of carbon films. The optical gap versus sp^2 percentage of a-C films prepared in this study is well matched with the reported literature [15]. The band gap also varies with the deposition techniques. Summarized band gap obtained from different deposition techniques is given in Table 4.

Table 2
XPS spectral data from as-grown and etched amorphous carbon films

Pyrolysis temperature (°C)	As-grown carbon film			Etched carbon film		
	C 1s peak position	Type of bonding	Atomic %	C 1s peak position	Type of bonding	Atomic %
650	289.4	C=O	1.6	287.7	C–O	9.6
	286.4	C–O	8.5	285.5	sp^3	58.0
	285.0	sp^3	25.5	284.8	sp^2	25.5
	284.6	sp^2	64.2			
750	288.6	C=O	2.5	287.7	C–O	6.7
	286.9	C–O	2.8	285.6	sp^3	47.4
	285.0	sp^3	28.3	284.7	sp^2	45.6
	284.6	sp^2	66.2			
900	287.9	C–O	1.4	288.9	C=O	2.9
	285.5	sp^3	17.7	285.9	sp^3	47.0
	284.6	sp^2	80.7	284.8	sp^2	50.0

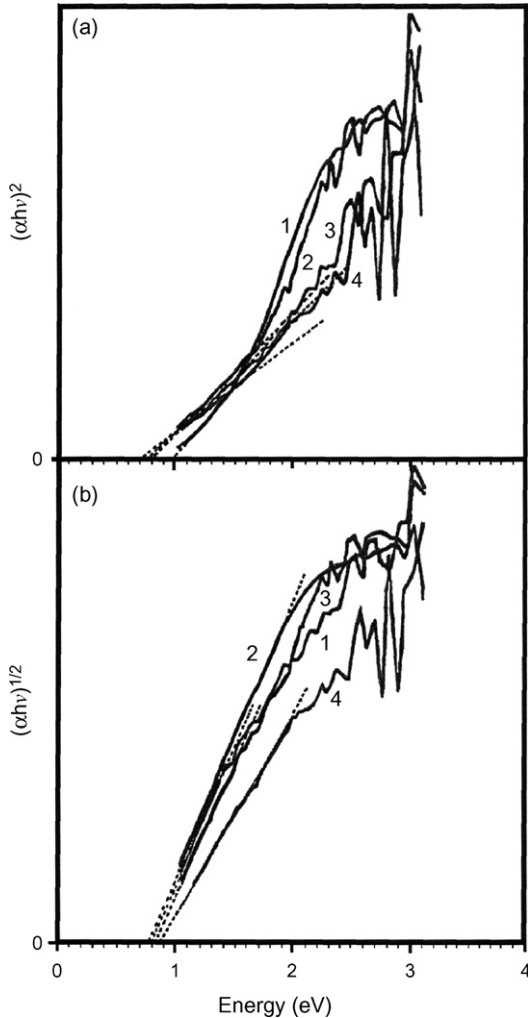


Fig. 3. Optical Tauc gap of a-C films deposited at different temperatures (a) direct band gap and (b) indirect band gap. Numerical number 1, 2, 3 and 4 in the spectra correspond to a-C films deposited at temperature of 650, 700, 750 and 900 °C, respectively.

3.4. Electrical properties

Electrical conductance versus temperature of a-C films (deposited at different temperatures) was measured as shown in Fig. 4. The study of electrical resistivity is one of the most important ways to address many issues concerning the electronic structure and properties of a-C films [45]. The theory of temperature dependence of resistivity is not same for a crystalline and an amorphous semiconductor. As per the conventional Mott–Davis model, the Fermi level (E_f) of an

Table 3
Optical band gaps of deposited carbon films

Deposition temperature (°C)	Optical band gap (eV)	
	Direct	Indirect
650	1.0–1.3	0.7–1.0
700	0.8–1.0	0.79
750	0.75	0.79
900	0.68	0.88

Table 4
Optical band gap of carbon films prepared by different methods

Samples	Optical gap (eV)
Graphite	0
a-C, evaporation [42]	0.4–0.7
a-C, sputtering [43]	0.4–0.74
a-C, pyrolysis (this work)	0.6–1.3
a-C, laser ablation [44]	0.6–1.7
a-C, arc [38]	2.1–2.4
Diamond	5.5

amorphous semiconductor protrudes as a peak in between valence band (VB) and conduction band (CB) as density of states $N(E_f)$ for charge carriers [46]. This peak is placed in the middle of the gap between VB and CB which normally originates from the defects, impurities, vacancies, etc. The electron states near the gap in a disorder system are either extended or localized. The imperfect gap is also called as pseudo gap or mobility gap, as localized state have zero mobility at 0 K. From the DOS calculation, it was found that σ – σ^* gap is wide and π – π^* gap is narrow [45]. In a-C, the π -states within σ -bands are highly localized. Details of the quantification of localized state and their reason of origin is discussed by Robertson [45]. As the films obtained in the present study are of amorphous type, Mott–Davis model was applied to electrical conductance plot (Fig. 4). In the Mott and Davis model [46], low temperature transport properties of a-C can be described in terms of variable range hopping (VRH) conductivity, as density of states present near the Fermi level. The carriers move between such states via phonon assisted tunneling and then tend to hop to a larger distance with decrease in temperature to find sites which are energetically closer than the nearest neighbor. This mechanism usually gives low thermoelectric power, which has been confirmed by thermoelectric power (TEP) measurements in the present study (discussed later). VRH method had been applied at low temperature by many authors and found to be suitable for the conductance plot [47]. In the VRH method:

$$\ln \sigma_{dc} = A - BT^{-1/4} \quad (3)$$

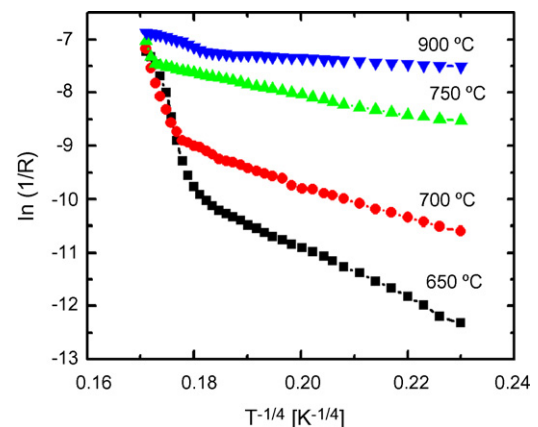


Fig. 4. Temperature dependence ($T^{-1/4}$) of $\ln \sigma$ for a-C films deposited at various temperatures.

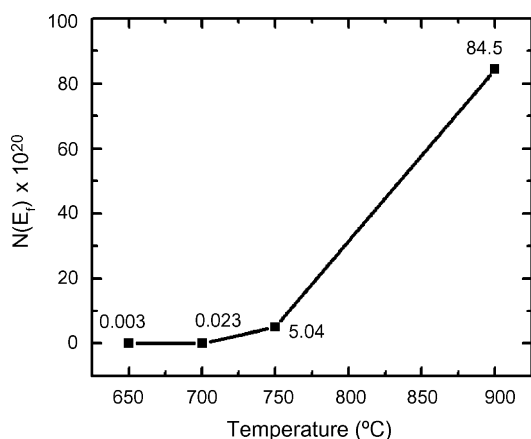


Fig. 5. Plot of $N(E_f)$ of a-C films vs. pyrolysis temperature.

where $B = \{16/a^3 kN(E_f)\}^{1/4}$, k is the Boltzman's constant, " a " is the radius of localized state wave function and $N(E_f)$ is the density of localized states at the Fermi level. So the slope of the straight lines carry the information of the product of " a " and " $N(E_f)$ ". By putting the conductance data into the VRH equation (3), it is found that fitting was not good in the whole temperature range (Fig. 4). In fact, for conductance measurement of the complete temperature range, the VHR mechanism is neither sufficient to give all answers nor well fitted to the whole temperature range [46,48].

Fig. 4 shows the plot of natural logarithm of conductance versus $T^{-1/4}$ (from Eq. (3)) of the a-C films prepared at different deposition temperatures. It was observed that conductance of a-C film increase with deposition temperature. The higher conductance of a-C films deposited at higher temperature (900 °C) was due to complete dissociation of precursor camphor and formation of more disorder sp^2 carbon sites, which resulted in the increase of localized hopping states. This increase of localized hopping states is reflected by the decrease in slopes angle with the increase in deposition temperature. In each a-C film, conductance increased with temperature and it shows two distinct slopes. In the lower temperature region, slope is of lower value than the higher temperature region. Lower temperature region of a-C films prepared at lower deposition temperature (650 °C) can be attributed to higher sp^3 or less disorderliness (as also observed in the Raman study). The higher conductance of same film in the high temperature region was due to formation of more disorderliness or sp^2 -bonded carbon. The increase of sp^2 states with temperature could lead to graphitization of the films making the $N(E_f)$ equal to $N_0(E_f)$ determined from $N_0(E_f) a^3 = 1$, so $N_0(E_f) = 6 \times 10^{20}$ states $(eV \text{ cm}^3)^{-1}$ for $a = 12 \text{ \AA}$. Here, $N(E_f)$ and $N_0(E_f)$ are density of states (DOS) of a-C film and graphite, respectively. The value of $N(E_f)$ has been calculated for all the films prepared at different deposition temperature taking $a = 12 \text{ \AA}$ of localized states with the assumption that " a " value remains constant [49,50]. Shimakawa and Miyake have calculated $N(E_f)$ taking $a = 10 \text{ \AA}$ in their films [51]. $N(E_f)$ was calculated to be 5.04×10^{20} $(eV \text{ cm}^3)^{-1}$ of the film

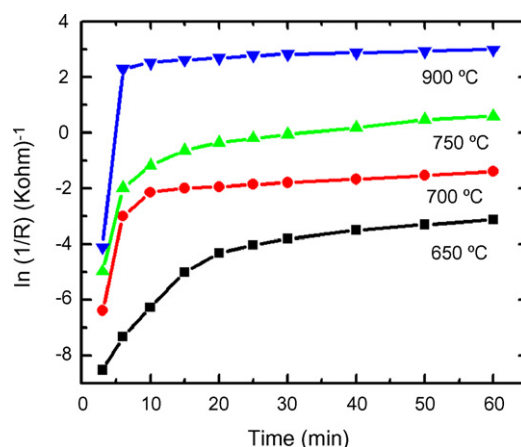


Fig. 6. Deposition time (min) vs. $\ln \sigma$ at various deposition temperatures.

prepared at 750 °C in the present work that matches exactly the theoretical value (taking $a = 12 \text{ \AA}$). At higher temperature (900 °C), this value crosses the theoretical value indicating its metallic nature. Fig. 5 shows $N(E_f)$ value versus temperature of deposition.

Above-mentioned study was carried out on the deposited a-C films. Electrical conductance was also measured while vaporization, pyrolysis of camphoric gas to carbon and deposition of carbon on substrate inside the reaction chamber. Fig. 6 shows the natural logarithm of conductance versus deposition time. The rapid increase in conductance in the first 10 min was due to the continuous deposition of more and more pyrolyzed carbon particles on the substrate as it normally took 6–12 min for complete vaporization of 2–3 g of camphor. As deposited carbon film kept for 1 h in the reaction chamber, a slow decrease in conductance after 10 min was due the effect of temperature. The conductance of the films was measured *in situ* while cooling from deposition temperature of 650 °C to room temperature, and was found to be reversible whereas further heating to more than 750 °C did not induce reversible trend. Conductance curve took a new irreversible path [48] which followed the same behavior to a-C film obtained at deposition temperature of 900 °C (Fig. 4).

3.5. Thermoelectric power (TEP) measurement

For an amorphous semiconductor, where carriers have a very short mean free path, Hall measurements are not as reliable as for conventional semiconductor. Therefore, measurements of thermoelectric power versus temperature difference provide a more direct way of determining whether the material is p- or n-type [46]. Fig. 7 shows thermoelectric power versus temperature of samples deposited at different temperatures. A positive thermoelectric power measured in present study ascertains the p-type nature of these films. The magnitude of thermoelectric power of a-C films is noticed to be larger than that of the graphite [52]. With increase in deposition temperature, there was a decrease in magnitude of thermoelectric power indicating that the films are proceeding towards metallic behavior (towards graphite).

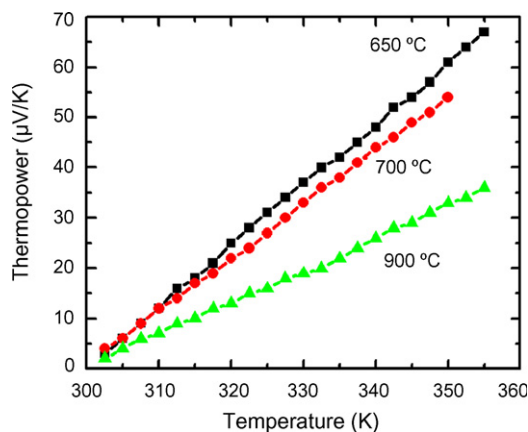


Fig. 7. Thermo-power of a-C films (deposited at different temperature) vs. temperature.

4. Conclusions

A novel and natural precursor camphor is used to synthesize a-C thin films. A simple method for preparing a-C thin films using high temperature thermal chemical vapor deposition process is presented and the physical properties of as grown a-C films are studied in detail. XRD shows these films are amorphous structure. XPS study demonstrates the variation of sp^3 and sp^2 percentages in the films deposited at various temperatures. Optical and electrical properties of a-C films varied significantly with deposition temperatures. The disorderliness and percentage of sp^2 -bonded carbon increases with deposition temperature and therefore, lower Tauc gap and higher conductivity of a-C films. However, all these films show p-type behavior in thermoelectric measurements.

Acknowledgements

The authors acknowledge free supply of camphor by Camphor Allied Limited, India in the present study. The authors are also thankful to Dr. Dominique Ballutaud, CNRS, France for XPS measurements.

References

- [1] S. Aisenberg, R. Chabot, *J. Appl. Phys.* 42 (1971) 2953.
- [2] S. Aisenberg, F.M. Kimock, in: J.J. Pouch, S.A. Alterovitz (Eds.), *Materials Science Forum, Properties and Characterization of Amorphous Carbon films*, vols. 52 and 53, Trans Tech. Publication, Switzerland, 1990 pp. 1–40.
- [3] R. Kalish, Y. Lifshitz, K. Nugent, S. Prawer, *Appl. Phys. Lett.* 74 (1999) 2936.
- [4] M.P. Siegal, P.N. Provencio, D.R. Tallant, R.L. Simpson, B. Kleinsorge, W.I. Milne, *Appl. Phys. Lett.* 76 (2000) 2047.
- [5] H. Kersten, G.M.W. Kroesen, *J. Vac. Sci. Technol. A* 8 (1990) 38.
- [6] M. Chowalla, J. Robertson, C.W. Chen, S.R.P. Silva, C.A. Davis, G.A.J. Amarantunga, W.I. Milne, *J. Appl. Phys.* 81 (1997) 139.
- [7] C. Casiraghi, A.C. Ferrari, J. Robertson, *Phys. Rev. B* 72 (2005) 85401.
- [8] B. Bhushan, J. Ruan, *Surf. Coat. Technol.* 68–69 (1994) 644.
- [9] J. Narayan, W.D. Fan, R.J. Narayan, P. Tiwari, H.H. Stadelmaier, *Mater. Sci. Eng. B* 25 (1994) 5.
- [10] K. Mukhopadhyay, I. Mukhopadhyay, M. Sharon, T. Soga, M. Umeno, *Carbon* 35 (1997) 863.
- [11] A.M.M. Omer, S. Adhikari, S. Adhikary, H. Uchida, M. Umeno, *Appl. Phys. Lett.* 87 (2005) 161912.
- [12] A. Ilie, A.C. Ferrari, T. Yagi, J. Robertson, *Appl. Phys. Lett.* 76 (2000) 2627.
- [13] H. Kiyota, M. Higashi, T. Kurosu, M. Iida, *J. Appl. Phys.* 99 (2006) 094903.
- [14] D. Pradhan, M. Sharon, *Electrochim. Acta* 50 (2005) 2905.
- [15] G. Adamopoulos, J. Robertson, N.A. Morrison, C. Godet, *J. Appl. Phys.* 96 (2004) 6348.
- [16] K. Mukhopadhyay, K.M. Krishna, M. Sharon, *Phys. Rev. Lett.* 72 (1994) 3182.
- [17] M. Sharon, K. Mukhopadhyay, K. Yase, S. Iijima, Y. Ando, X. Zhao, *Carbon* 36 (1998) 507.
- [18] M. Kumar, K. Kakamu, T. Okazaki, Y. Ando, *Chem. Phys. Lett.* 385 (2004) 161.
- [19] D. Pradhan, M. Sharon, M. Kumar, Y. Ando, *J. Nanosci. Nanotechnol.* 3 (2003) 215.
- [20] M. Sharon, D. Pradhan, *J. Nanosci. Nanotechnol.* 5 (2005) 1718.
- [21] Q. Wu, L. Yu, Y. Ma, Y. Liao, R. Fang, L. Zhang, X. Chen, K. Wang, *J. Appl. Phys.* 93 (2003) 94.
- [22] C. Ramaswamy, *Nature* 125 (1930) 704.
- [23] S.A. Solin, A.K. Ramdas, *Phys. Rev. B* 1 (1970) 1687.
- [24] J. Robertson, *Adv. Phys.* 35 (1986) 317.
- [25] P.K. Bachmann, D.U. Wiechert, in: R.E. Clausing, L.L. Horton, J.C. Angus, P. Koidl (Eds.), *Diamond and Diamond-Like Films and Coatings*, NATO ASI series, vol. 266, Plenum Press, New York, 1991, pp. 677–713.
- [26] A.C. Ferrari, J. Robertson, *Phys. Rev. B* 61 (2000) 14095.
- [27] R.E. Shroder, R.J. Nemanich, J.T. Glass, *Phys. Rev. B* 41 (1990) 3738.
- [28] J. Kulik, G.D. Lempert, E. Grossman, D. Marton, J.W. Rabalais, Y. Lifshitz, *Phys. Rev. B* 52 (1995) 15812.
- [29] A. Hoffman, A. Heiman, H.P. Strunk, S.H. Christiansen, *J. Appl. Phys.* 91 (2002) 3336.
- [30] F. Tuinstra, J.L. Koenig, *J. Chem. Phys.* 53 (1970) 1126.
- [31] M.A. Tarmor, J.A. Haire, C.H. Wu, K.C. Hass, *Appl. Phys. Lett.* 54 (1989) 123.
- [32] F. Li, J.S. Lannin, *Appl. Phys. Lett.* 61 (1992) 2116.
- [33] J.K. Shin, C.S. Lee, K.R. Lee, K.Y. Eun, *Appl. Phys. Lett.* 78 (2001) 631.
- [34] M. Hanfland, H. Beister, K. Syassen, *Phys. Rev. B* 39 (1989) 12598.
- [35] J.O. Orwa, I. Andrienko, J.L. Peng, S. Prawer, Y.B. Zhang, S.P. Lau, *J. Appl. Phys.* 96 (2004) 6286.
- [36] J. Diaz, G. Paolicelli, S. Ferrer, F. Comin, *Phys. Rev. B* 54 (1996) 8064.
- [37] D. Briggs, M.P. Seah, *Progress in Surface Analysis*, vol. 1, Auger and X-ray Photoelectron Spectroscopy, Wiley, Chichester, UK, 1990, pp. 599 and 606.
- [38] R. Lossy, D.L. Pappas, R.A. Roy, J.J. Cuomo, V.M. Sura, *Appl. Phys. Lett.* 61 (1992) 171.
- [39] J. Robertson, E.P. O'Reilly, *Phys. Rev. B* 35 (1987) 2946.
- [40] J. Robertson, *Diam. Relat. Mater.* 4 (1995) 297.
- [41] D.A. Drabold, P.A. Fedders, P. Stumm, *Phys. Rev. B* 49 (1994) 16415.
- [42] J. Robertson, *Diamond and Diamond-like Carbon Films*, NATO Advanced Study Institute, New York, 1991.
- [43] N. Savvides, B. Window, *J. Vac. Sci. Technol. A* 3 (1985) 2386.
- [44] J.J. Cuomo, D.L. Pappas, J. Bruley, J.P. Doyle, K.L. Saenger, *J. Appl. Phys.* 70 (1991) 1706.
- [45] J. Robertson, *Mater. Sci. Eng. R* 37 (2002) 129.
- [46] N.F. Mott, E.A. Davis, *Electronic Processes in Non-Crystalline Materials*, Clarendon Press, London, 1979.
- [47] J.J. Hauser, *J. Non-Cryst. Solids* 23 (1977) 21.
- [48] J.J. Hauser, *Solid State Commun.* 17 (1975) 1577.
- [49] J.J. Hauser, J.R. Patel, J.W. Rodgers, *Appl. Phys. Lett.* 30 (1977) 129.
- [50] F. Fontaine, E. Gheeraert, A. Deneuille, *Diam. Relat. Mater.* 5 (1996) 752.
- [51] K. Shimakawa, K. Miyake, *Phys. Rev. Lett.* 61 (1988) 994.
- [52] T. Takezawa, T. Tsuzuku, A. Ono, Y. Hishiyama, *Phil. Magn.* 19 (1969) 623.